Theory of a density-wave instability in symmetric nuclear matter

A. E. Pozamantir and A. W. Overhauser
Department of Physics, Purdue University, West Lafayette, Indiana 47907-1396
(Received 29 July 1999; published 4 June 2001)

Symmetric nuclear matter is found to have a spontaneously broken translational symmetry. This collective instability creates a one-dimensional nucleon density wave of periodicity 15–27 fm, with a peak-to-trough density ratio ~6. As a result, the binding energy of the system increases by 0.5–1.5 MeV per nucleon relative to that for uniform nuclear matter. The latter must therefore be regarded as a highly excited metastable state.

DOI: 10.1103/PhysRevC.64.014303 PACS number(s): 21.65.+f, 21.60.Ev, 21.60.Jz, 21.10.Dr

I. INTRODUCTION

The possibility that symmetric nuclear matter (equal proton and neutron densities) may develop a spontaneously broken translational symmetry was introduced in 1960 [1]. The simplest example is a single nucleon density wave (NDW). If the wave vector of the modulation is $Q\hat{z}$, the nucleon density variation will be

$$\rho \cong \rho_0(1+\gamma\cos Qz), \tag{1}$$

where ρ_0 is the (optimum) mean density of nuclear matter and, of course, $\gamma<1$,

$$\rho_0=\left(\frac{4\pi}{3}R_0^3\right)^{-1}=0.179\,\mathrm{fm}^{-3}, \tag{2}$$

the value obtained if the nuclear radius for mass A is $R_0A^{1/3}$ and if, as is frequently chosen, $R_0=1.10$ fm. It follows that the Fermi-sphere radius of the degenerate Fermi sea is $k_F=1.38\,\mathrm{fm}^{-1}$.

The simplest path for understanding the origin of an NDW, Eq. (1), is to redistribute the nucleons that fill the Fermi sphere so that, instead, they fill a cylinder (of equal volume) having diameter D and length Q. [The circular faces of the cylinder cut the k_z axis at $k_z=\pm(1/2)Q$.] The kinetic-energy increase caused by this repopulation, ~1.0 MeV per nucleon, is a minimum when $D=2Q/\sqrt{3}$. An NDW can now arise spontaneously if the nucleon wave functions are allowed to acquire momentum components, $\vec{k}\pm\vec{Q}$, where $\vec{Q}=Q\hat{z}$. For $k_z>0$,

$$|\vec{k}\rangle \rightarrow |\vec{k}\rangle + c(k_z)|\vec{k}-\vec{Q}\rangle + d(k_z)|\vec{k}+\vec{Q}\rangle. \tag{3}$$

(For $k_z<0$, the coefficients c and d are interchanged.) One should note that the filled states, $|\vec{k}\rangle$, are admixed only with empty states, $|\vec{k}\pm\vec{Q}\rangle$. The Hartree-Fock (HF) energy of this many-nucleon configuration can be optimized by an appropriate choice of $c(k_z)$ and $d(k_z)$ [1]. These admixtures cause an additional increase in kinetic energy, proportional to the square of the resulting NDW amplitude γ,

$$\Delta\langle T\rangle \sim \gamma^2. \tag{4}$$

In contrast, the expectation value, $\langle V\rangle$, of the nucleon-nucleon interaction becomes more negative,

$$\Delta\langle V\rangle \sim -\gamma^2 \ln\left(\frac{1}{\gamma}\right). \tag{5}$$

Since γ, and therefore $\ln(1/\gamma)$, can always be chosen so that Eq. (5) dominates Eq. (4), a cylindrical Fermi surface will always support an NDW. The original estimate of $\Delta\langle T\rangle+\Delta\langle V\rangle$ was ≈ -1.3 MeV per nucleon [1], a value that exceeds the 1.0 MeV kinetic energy increase required to repopulate k space. Consequently it seemed reasonable to suppose that infinite nuclear matter might support a broken symmetry.

However, there is a flaw in the foregoing argument. The energy increase required to repopulate momentum space (from a sphere to a cylinder) is considerably more than the 1.0 MeV already mentioned. Consider the repulsive core of the nucleon-nucleon interaction (which is responsible for the saturation of nuclear forces). Greater penetration of the repulsive core occurs whenever the kinetic energy of pairwise relative motion increases. Consequently there will be an increase in $\langle V\rangle$ resulting from the initial k-space repopulation. The outcome of the competition between the repulsive and attractive terms becomes less certain.

To study the situation in more detail, one has to adopt a nucleon-nucleon (phenomenological) interaction. A basic requirement for the potential is not only to reproduce the essential properties of symmetric nuclear matter (binding energy, equilibrium density, etc.) but also the binding energies of finite symmetric nuclei (^{4}He, ^{16}O, ^{40}Ca, etc.). Clearly, if finite symmetric nuclei acquire more binding energy per nucleon than symmetric nuclear matter, the latter will inevitably break up into finite nuclei. The binding energy of the resulting configuration can be increased further by bringing these nuclei closer to each other, so that their nucleon densities partially overlap. Studies show that even in the case of slightly overbound finite nuclei, the tendency to form this fictitious ''quasicrystallization'' is present.

In the present study we use a recently proposed finite-range phenomenological nucleon-nucleon potential [2] that has the form

$$V(\mathbf{r}_1,\mathbf{r}_2)=-\alpha C(\mathbf{r}_1-\mathbf{r}_2)^2 e^{-(\mathbf{r}_1-\mathbf{r}_2)^2/s^2}+\beta\sqrt{\langle T\rangle}\,\delta(\mathbf{r}_1-\mathbf{r}_2), \tag{6}$$

where $\langle T\rangle$ is the (center-of-mass-motion corrected) average kinetic energy given by

$$\langle T\rangle=\frac{1-1/A}{A}\sum_{i=1}^{A} t_i, \tag{7}$$

with t_i being the kinetic energy of the ith nucleon, and $A=2N=2Z$, the total number of nucleons: C is the normalization coefficient of the modified Gaussian

$$C=(\tfrac{3}{2}\pi^{3/2}s^5)^{-1}. \tag{8}$$

Saturation of nuclear forces is achieved by letting the n-n repulsion increase with increasing $\langle T\rangle$. The three parameters of the potential are chosen as

$$\alpha=1690\ \text{MeV fm}^3,\quad \beta=255\ \text{MeV}^{1/2}\ \text{fm}^3,\quad s=0.54\ \text{fm}. \tag{9}$$

For the case of symmetric nuclear matter ($A\to\infty$), the average kinetic energy per nucleon is calculated by integration over the occupied modes in the Fermi sea, as explained in the following section.

The determination of the nucleon-nucleon potential (6) and its properties are discussed in Ref. [2]. The potential gives satisfactory values for binding energies of light symmetric nuclei. For uniform symmetric nuclear matter it yields the binding energy per nucleon, $B_0=15\,\text{MeV}$, the mean nuclear density, $\rho_0=0.179\,\text{fm}^{-3}$, the compressibility modulus, $K=225\,\text{MeV/fm}^3$ and the nucleon effective mass, $\mu^*/\mu=0.41$.

The reason for our decision to choose the parameters (9) so that B_0 (for uniform nuclear matter) is $\sim$1 MeV less than a commonly accepted value, $\sim$16 MeV/nucleon, is the subject of this study. It will be shown that symmetric nuclear matter does support an NDW. This broken-symmetry state gives rise to an additional $\sim$1 MeV/nucleon of binding energy, compared with uniform nuclear matter. Preliminary studies (Sec. II) show that, instead of a large-wave-vector (small wavelength) NDW ($Q\sim 2k_F$), that one might have expected, nuclear matter favors a small-wave-vector NDW, $Q<(1/4)k_F$. The theory of a small-Q NDW in three-dimensional symmetric nuclear matter is presented in Sec. III. The variational technique employed in the HF calculations is elaborated in Sec. IV. Results are presented in Sec. V. Implications for finite nuclei are discussed in Sec. VI.

II. PRELIMINARY STUDIES

A three-dimensional periodic nuclear density could arise as the result of a periodic arrangement of nucleons in a three-dimensional lattice. Of all possible spatial lattices, the ground state of such a nucleon crystal would correspond to the one that maximizes the binding energy of the system. If symmetric nuclear matter were to exhibit a three-dimensional (3-D) density instability, a natural choice would be an arrangement of nucleons in a face-centered-cubic (fcc) lattice. Each lattice cell would contain four nucleons: two protons, spin-up and spin-down, and two neutrons, spin-up and spin-down. (For comparison, the average kinetic energy per nucleon in the filled Brillouin zone of fcc, bcc, and simple cubic lattices is 1.020, 1.023, and 1.083, respectively, in units of the average kinetic energy of a filled Fermi sphere having equal k-space volume.) One can adjust the lattice constant a so that the occupied states fill entirely the first Brillouin zone (in momentum space). The first Brillouin zone (FBZ) of an fcc lattice has eight faces with orientation indices {111}, and six faces with orientation indices {200}. The existence of flat boundaries between occupied and empty states is conducive to a large wave-vector ($\sim 2k_F$) instability that mixes filled states inside the boundaries with empty states outside, but across the Fermi sea. The ''penalty'' in kinetic energy increase is then a minimum. The one-particle orbital wave functions are

$$\varphi_{ijk}(\mathbf{r})=N\sum_{\mathbf{G}} f_{\mathbf{k},\mathbf{G}}e^{i(\mathbf{k}+\mathbf{G})\cdot\mathbf{r}}. \tag{10}$$

The indices, $\{ijk\}$, describe the wave vector $\mathbf{k}$. The summation is over all reciprocal lattice vectors [i.e., $\mathbf{G}=0$, $\mathbf{G}=(\pm1\pm1\pm1)$, $\mathbf{G}=(\pm200)$, etc.]. We will treat $f_{\mathbf{k},\mathbf{G}}$ as variational coefficients. N is a normalization coefficient.

If only the {111} and {200} families of the mixing wave vector $\mathbf{G}$ (including $\mathbf{G}=0$) are considered, the nucleon density can be written as

$$\rho=\frac{16}{a^3}\sum_{l,m,n} g_{lmn}\cos(lGx+mGy+nGz),$$

where the summation indices, $\{l,m,n\}$, range over the following values: (0,0,0), ($\pm$1,1,1), (2,0,0), ($\pm$2,2,0), ($\pm$3, $\pm$1,1), ($\pm$2,2,2), and (4,0,0) with all possible permutations within the parenthesis. $g_{l,m,n}$ are the strengths of the different Fourier harmonics, and are expressed through various combinations of the coefficients $f_{\mathbf{k},\mathbf{G}}$ of Eq. (10). The coefficients $g_{l,m,n}$ are symmetric with respect to the sign and index permutations; a is the fcc lattice constant. The HF interaction energy per nucleon calculated from the potential (6) is (with $g_{000}=1$):

$$\begin{aligned}U=&-\frac{4}{a^3}\alpha[1-g_s(\langle T\rangle)]\times[2+4g_{111}^2(1-\tfrac{1}{2}x)\\&\times e^{-3/4x}+3g_{200}^2(1-\tfrac{2}{3}x)e^{-x}+6g_{220}^2(1-\tfrac{4}{3}x)e^{-2x}\\&+12g_{311}^2(1-\tfrac{11}{6}x)e^{-11/4x}+4g_{222}^2(1-2x)e^{-3x}\\&+3g_{400}^2(1-\tfrac{8}{3}x)e^{-4x}]+\frac{3}{a^3}\beta\sqrt{\langle T\rangle}(2+4g_{111}^2+3g_{200}^2\\&+6g_{220}^2+12g_{311}^2+4g_{222}^2+3g_{400}^2).\end{aligned} \tag{11}$$

The term in the first square brackets is the exchange energy correction calculated in the statistical approximation [2]. The dimensionless parameter x is defined as

$$x\equiv\left(\frac{2\pi s}{a}\right)^2, \tag{12}$$

where s is the range parameter of the potential (6). Numerical studies show that, in order to overcome the additional repulsion and to obtain an increase in binding energy, the form factor for the attractive potential at the first Fourier component g_{111} has to be larger than $\sim$0.7:

$$(1-\tfrac{1}{2}x)e^{-3/4x}\approx 0.7.$$

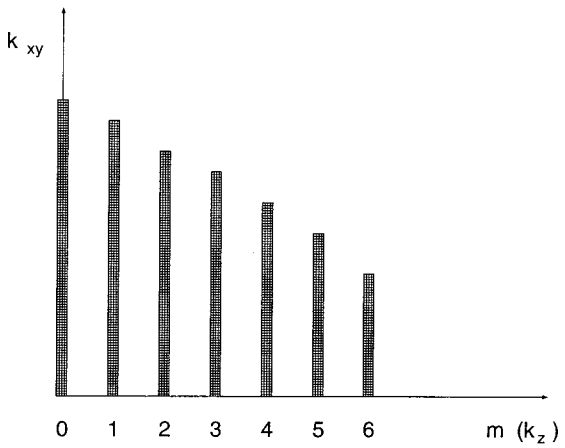

FIG. 1. The calculated Fermi radii of the 2-D nucleon seas for a Gaussian slab of modality seven with no mixing of oscillator wave functions. The largest radius, $k_{F_0}=1.47\ \mathrm{fm}^{-1}$, and the smallest, $k_{F_0}=0.62\ \mathrm{fm}^{-1}$. It turns out that $m=6$ is the highest occupied 1-D oscillator mode for the ground state of the slab.

This relation requires $x\approx 0.3$, or $a\approx 6$ fm. One has to compare this value of a with the corresponding lattice constants of face-centered, body-centered, and simple cubic lattices (having four nucleons in each primitive unit cell):

$$a_{\mathrm{fcc}}=\left(\frac{16}{\rho_0}\right)^{1/3}=4.47\ \mathrm{fm},\quad a_{\mathrm{bcc}}=\left(\frac{8}{\rho_0}\right)^{1/3}=3.55\ \mathrm{fm},$$

$$a_{\mathrm{sc}}=\left(\frac{4}{\rho_0}\right)^{1/2}=2.82\ \mathrm{fm}.$$

An NDW is possible only if the lattice parameter of the periodic nuclear structure is much larger than these anticipated values. If the range of the attractive potential is much smaller than 0.5 fm, a short-period density-wave instability can occur. However, such an instability is spurious; the problem with a short-range attractive potential is that the binding energy per nucleon of ^{4}He then exceeds that of nuclear matter, which could then spontaneously break up into individual α particles.

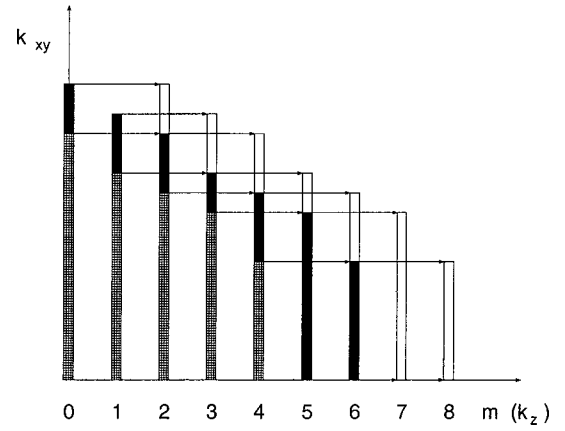

FIG. 2. The calculated Fermi radii of the 2-D Fermi seas for a Gaussian slab of modality seven. The mixing involves states for which k_m is larger than $k_{F_{m+2}}$. These states are black. The empty states utilized in the mixing are shown in white. The last two occupied modes, $m=5,6$, are mixed with modes $m=7,8$, without restriction on k_m. The mixing preserves the parity of each mode.

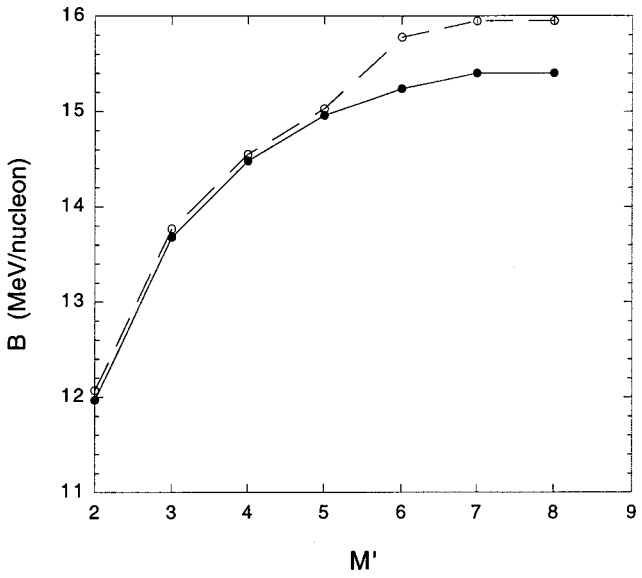

FIG. 3. The binding energy (absolute value) per nucleon vs modality M' in a Gaussian slab of symmetric nuclear matter for pure one-dimensional oscillator states (solid line) and for mixed oscillator states (dashed line). Both curves saturate at $M'=7$.

If one examines a 3-D density-wave instability with a small Q, $Q=2\pi/a<2k_F$, the Fermi surface becomes a multifaceted polyhedron. Furthermore, the nucleon orbitals become linear combinations of an extraordinarily large number of plane waves. The following study will, for simplicity, be confined to a single NDW (in 3-D nuclear matter). As a preparation, we will consider first a slab of nuclear matter,

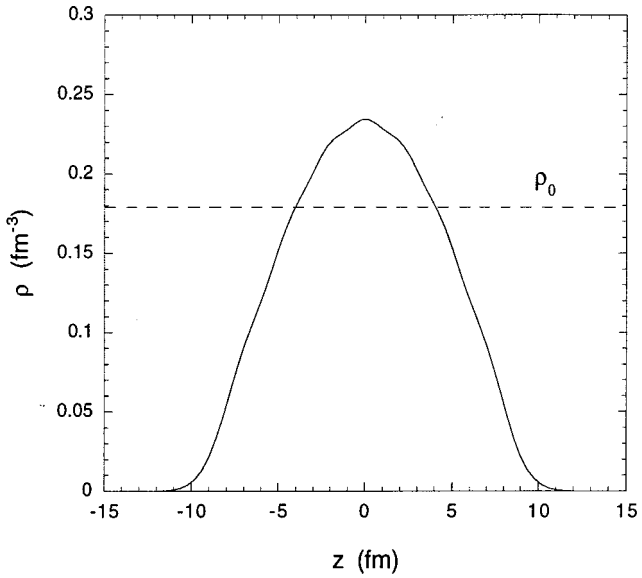

FIG. 4. Density profile along the z axis of a Gaussian slab of nuclear matter for modality $M'=7$ with no wave-function mixing. The dashed line indicates the equilibrium density of nuclear matter.

uniform in the (x, y) plane, but localized in the $\hat{z}$ direction. Let us assume the nucleon orbitals will be products of 2-D plane waves (in the $\hat{x}$ and $\hat{y}$ directions) and harmonic oscillator wave functions (in the $\hat{z}$ direction):

$$\psi^0_{\mathbf{k},m}(\boldsymbol{\rho},z)=Ne^{i\mathbf{k}\cdot\boldsymbol{\rho}}\varphi_m(z). \tag{13}$$

Here N is a normalization constant for the plane wave; the one-dimensional oscillator wave functions, $\varphi_m(z)$, are normalized; $\boldsymbol{\rho}$ is the (x, y) plane coordinate, and $\mathbf{k}$ is the wave vector associated with motion in the (x, y) plane. Assume that the oscillator states with $m=0,1,...,M$ are occupied, while the states with $m>M$ are empty. The number, $M'=M+1$, we call modality, and is the number of oscillator levels involved in occupied states. We define the fractional occupancy A_m of each oscillator mode m as the ratio of the number of particles in this mode to the total number of nucleons in the system. The fractional occupancies $A_0,A_1,\ldots,A_M$ obey the obvious constraint

$$\sum_{m=0}^{M} A_m=1. \tag{14}$$

When the nuclear slab is in its ground state, $A_0>A_1>\cdots>A_M$. Therefore, the Fermi momenta, k_{F_m}, of the M' two-dimensional Fermi seas satisfy

$$k_{F_0}>k_{F_1}>\cdots>k_{F_M}, \tag{15}$$

as shown in Fig. 1 for the case $M'=7$.

We now introduce greater variational freedom for the oscillator modes by the mixing illustrated in Fig. 2. If a nucleon in the mth mode has a wave vector $\mathbf{k}$ such that $k>k_{F_{m+2}}$, its wave function is taken to be the sum of two components of type (13), namely, those for m and $m'=m+2$, both of the same $\mathbf{k}$. The resulting wave function has the same parity as its components.

$$\psi^0_{\mathbf{k},m}\rightarrow\psi_{\mathbf{k},m}=\begin{cases}\psi^0_{\mathbf{k},m}, & \text{if } k_m\leqslant k_{F_{m+2}}\\ \dfrac{1}{\sqrt{1+c_m^2}}(\psi^0_{\mathbf{k},m}+c_m\psi^0_{\mathbf{k},m+2}), & \text{if } k_m>k_{F_{m+2}},\end{cases} \tag{16}$$

for $m=0,1,...,M-2$, and

$$\psi^0_{\mathbf{k},m}\rightarrow\psi_{\mathbf{k},m}=\frac{1}{\sqrt{1+c_m^2}}(\psi^0_{\mathbf{k},m}+c_m\psi^0_{\mathbf{k},m+2}), \quad \text{for any } k_m \tag{17}$$

when $m=M-1$, M. The availability of empty states in the m'th mode required for this mixing follows from Eq. (15), while mixing of the last two modes, $M-1$ and M, with unoccupied modes, $M+1$ and $M+2$, has no restriction on k_m. The mixing coefficients, c_m, are variables in the Hartree-Fock procedure. The energy functional (binding energy per nucleon in the slab), B, is calculated in the Appendix and depends on $2M'+1$ variables:

$$B=B(\eta,\rho_G;A_1,A_2,\ldots,A_M;c_0,c_1,\ldots,c_M). \tag{18}$$

The density parameter, ρ_G, is defined in the Appendix, Eq. (A4). η is the exponential decay parameter that appears in the harmonic oscillator wave functions. Its value determines the thickness of the slab.

If the mixing coefficients, c_m, are set to zero in Eq. (18), the binding energy B versus modality M' saturates at $M'=7$ with $B=15.4$ MeV/nucleon. This behavior is shown in Fig. 3. Allowing the next mode, $m=7$, to be occupied does not lead to a new result. k_{F_7} turns out to be zero, so the nucleon distribution among the first seven modes remains identical to the $M'=7$ case. (There is, of course, no further increase in B.) The density profile along the z axis of the slab (without mixing) for $M'=7$ is shown in Fig. 4.

The binding energy increases when one introduces the mixing coefficients as variational parameters. Variation of Eq. (18) with respect to all $2M'+1$ variables leads to nonzero values for all c_m. The binding energy is enhanced relative to the pure Gaussian slab, as shown in Fig. 3. The limiting case is again, $M'=7$, and $B=15.9$ MeV/nucleon. The nuclear density along the z axis, expressed in terms of the one-dimensional oscillator states φ_m is

$$\begin{aligned}\rho(z)=\rho_G\left(\frac{2\pi}{\eta}\right)^{1/2}\Bigg[&A_2\varphi_0(z)^2+\frac{A_0-A_2}{1+c_0^2}[\varphi_0(z)+c_0\varphi_2(z)]^2+A_3\varphi_1(z)^2+\frac{A_1-A_3}{1+c_1^2}[\varphi_1(z)+c_1\varphi_3(z)]^2+A_4\varphi_2(z)^2\\&+\frac{A_2-A_4}{1+c_2^2}[\varphi_2(z)+c_2\varphi_4(z)]^2+A_5\varphi_3(z)^2+\frac{A_3-A_5}{1+c_3^2}[\varphi_3(z)+c_3\varphi_5(z)]^2+A_6\varphi_4(z)^2+\frac{A_4-A_6}{1+c_4^2}[\varphi_4(z)+c_4\varphi_6(z)]^2\\&+\frac{A_5}{1+c_5^2}[\varphi_5(z)+c_5\varphi_7(z)]^2+\frac{A_6}{1+c_6^2}[\varphi_6(z)+c_6\varphi_8(z)]^2\Bigg],\end{aligned} \tag{19}$$

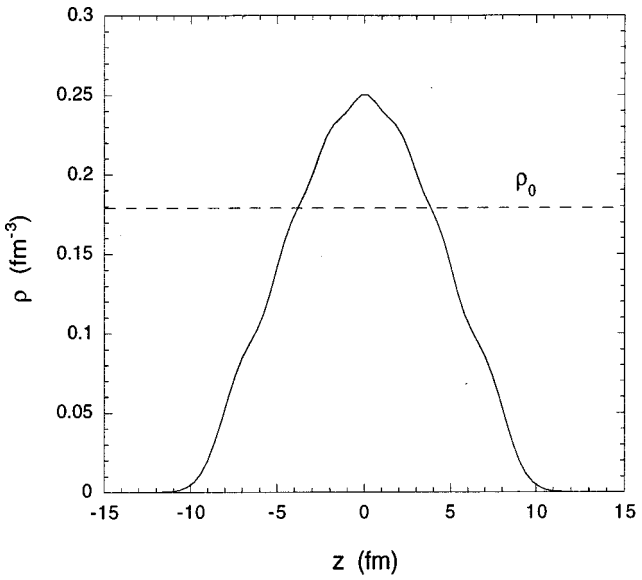

FIG. 5. Density profile along the z axis of a Gaussian slab of nuclear matter for modality $M'=7$ with wave-function mixing. The dashed line indicates the equilibrium density of nuclear matter.

and is shown in Fig. 5. The appearance of the factors $(A_m - A_{m+2})$ in this formula can be readily understood by observing that the number of nucleons involved in the mixing for each mode, m, is proportional to the difference in Fermi disk areas for the mth and $(m+2)$th modes, as illustrated in Fig. 6.

These results already show that uniform (symmetric) nuclear matter is unstable. It can break up into Gaussian slabs with $M'=7$ and gain 0.9 MeV extra binding. Obviously, the binding energy could be increased further by bringing these slabs close to each other such that the adjacent densities slightly overlap. An infinite array of such overlapping slabs would form a periodic structure having a lower energy than that of uniform nuclear matter. The theory of a single NDW is presented in the following section.

III. NDW IN NUCLEAR MATTER: THEORY

In view of the result of the previous section, one would be tempted to build three-dimensional nuclear matter from a collection of two-dimensional Gaussian slabs having a periodicity a. Such an approach would be very cumbersome. We will continue to assume that the wave functions in the (x, y) plane are pure plane waves. However, the z components of the basis functions must be Bloch functions instead of harmonic oscillator ones:

$$\psi_{\mathbf{k}_\perp, k_z}(\boldsymbol{\rho}, z) = N e^{i\mathbf{k}_\perp \cdot \boldsymbol{\rho}} \varphi_{k_z}(z). \tag{20}$$

According to Bloch's theorem, one-dimensional periodic wave functions, $\varphi_{k_z}(z)$, have the form

$$\varphi_{k_z}(z) = e^{ik_z z} u_{k_z}(z). \tag{21}$$

The periodic function, $u_{k_z}(z)$, can be expanded in a Fourier series,

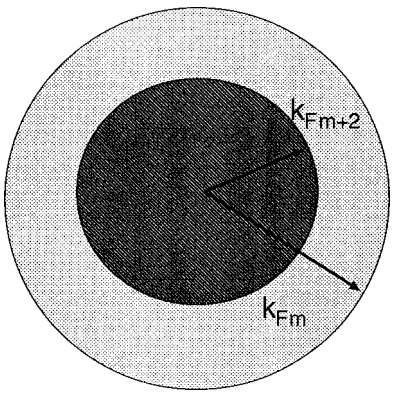

FIG. 6. The number of nucleons in each mode m that undergo mixing is proportional to the difference in areas of the Fermi disks corresponding to the mth and $(m+2)$th modes.

$$u_{k_z}(z) = \sum_j h_j e^{iG_j z}, \tag{22}$$

where G_j are reciprocal lattice vectors. Here, however, $G_j = 2\pi j/a$, and all are parallel to $\hat{z}$.

For computational convenience we introduce discrete values for k_z, distributed symmetrically around $k_z = 0$:

$$k_z \rightarrow \frac{m}{\Gamma} Q, \quad m = \pm\frac{1}{2}, \ \pm\frac{3}{2}, \ \pm\frac{5}{2}, \ldots, \ \pm\frac{\Gamma-1}{2}. \tag{23}$$

Here Γ (an even number) is the number of k_z values in each Brillouin zone (BZ). (We found that, $\Gamma = 14$, is a sufficiently fine net for our purposes.) The reciprocal lattice vectors (scalars here) are

$$G_j = 0, \pm Q, \pm 2Q, \pm 3Q, \ldots, \tag{24}$$

where Q is the size of the (one-dimensional) BZ,

$$Q = \left(\frac{2\pi}{a}\right). \tag{25}$$

In practice, to limit the computational load, we restrict our attention to

$$4Q \leqslant |G_{j\,\max}| \leqslant 7Q. \tag{26}$$

The Bloch functions (21) become

$$\varphi_m(z) = e^{imQz/\Gamma}(\cdots + a_m e^{-i2Qz} + b_m e^{-iQz} + c_m + d_m e^{iQz} + f_m e^{i2Qz} + \cdots). \tag{27}$$

Each of the states (27) is an admixture of as many as 15 $(G_{j\,\max} = 7Q)$ plane waves. The mixing coefficients: $\ldots, a_m, b_m, d_m, f_m, \ldots$ as well as the BZ size Q are variational parameters in the Hartree-Fock procedure.

A simple approach to generate orthonormal one-particle states, such as Eq. (27), is to perturb the free-nucleon (plane wave) states by a periodic potential of periodicity Q. The new nucleon orbitals are then eigenvectors of the following quasidiagonal (symmetric) pseudo-Hamiltonian:

$$\frac{\hbar^2}{2\mu}\begin{pmatrix} \cdots & \cdots & \cdots & & & & \\ & (k-2Q)^2 & G(k) & H(k) & & & \\ & G(k) & (k-Q)^2 & G(k) & H(k) & & \\ & H(k) & G(k) & k^2 & G(k) & H(k) & \\ & & H(k) & G(k) & (k+Q)^2 & G(k) & \\ & & & H(k) & G(k) & (k+2Q)^2 & \\ & & & & \cdots & \cdots & \cdots \end{pmatrix},$$

written in a truncated plane-wave basis of free nucleons. The only nonzero off-diagonal terms, G and H, simulate the first and second harmonics of a periodic pseudopotential. They mix states having wave vectors that differ by Q and $2Q$, respectively. (Calculations show that, while the second harmonic plays an important role in the subsequent density instability, inclusion of higher harmonic terms in the Hamiltonian does not change the results drastically.) In accordance with Eq. (26), the dimension of the Hamiltonian matrix in our calculations was chosen between 9×9 and 15×15. The wave vector k [see Eq. (23)] is limited to the first Brillouin zone. This situation is illustrated in Fig. 7 for the case, $\Gamma=6$ with three zones fully occupied. (Both extended and reduced BZ schemes are shown.) In the reduced BZ scheme, G and H cause ''vertical'' mixing (shown by vertical arrows in the reduced BZ scheme in Fig. 7) between the plane-wave states. The effective Hamiltonian, if truncated at 5×5, is

$$\frac{\hbar^2}{2\mu}\left(\frac{Q}{\Gamma}\right)^2\begin{pmatrix} (m-2\Gamma)^2 & G_m & H_m & 0 & 0 \\ G_m & (m-\Gamma)^2 & G_m & H_m & 0 \\ H_m & G_m & m^2 & G_m & H_m \\ 0 & H_m & G_m & (m+\Gamma)^2 & G_m \\ 0 & 0 & H_m & G_m & (m+2\Gamma)^2 \end{pmatrix}, \quad m=\frac{1}{2};\frac{3}{2};\frac{5}{2}.$$

Upon diagonalization, with $m=1/2$, the new (orthogonal) wave functions will have wave-vector indices α, given by m, $m\pm6$, $m\pm12$:

$$\alpha=-\tfrac{23}{2};-\tfrac{11}{2};\tfrac{1}{2};\tfrac{13}{2};\tfrac{25}{2} \quad (m=\tfrac{1}{2}). \tag{28}$$

Only three of these values will correspond to occupied states (see Fig. 7):

$$\alpha=-\tfrac{11}{2};\tfrac{1}{2};\tfrac{13}{2} \quad (m=\tfrac{1}{2}). \tag{29}$$

Similarly, the wave functions for the other occupied states are obtained by diagonalizing the matrix for each of the remaining m values,

$$\alpha=-\tfrac{9}{2};\tfrac{3}{2};\tfrac{15}{2} \quad (m=\tfrac{3}{2}), \tag{30}$$

and

$$\alpha=-\tfrac{7}{2};\tfrac{5}{2};\tfrac{17}{2} \quad (m=\tfrac{5}{2}). \tag{31}$$

Making use of time-reversal symmetry, $\varphi_{-\alpha}(z)=\varphi_\alpha^*(z)$, one obtains a full set of orthonormal one-dimensional Bloch functions, normalized in an interval of length, L:

$$\varphi_\alpha(z)=L^{-1/2}K_\alpha e^{i\alpha Qz/\Gamma}(a_\alpha e^{-\iota 2Qz}+b_\alpha e^{-\iota Qz}+c_\alpha+d_\alpha e^{\iota Qz}+f_\alpha e^{\iota 2Qz}), \tag{32}$$

$$K_\alpha\equiv(a_\alpha^2+b_\alpha^2+c_\alpha^2+d_\alpha^2+f_\alpha^2)^{-1/2}, \quad \alpha=\tfrac{1}{2};\ldots;\tfrac{17}{2}, \tag{33}$$

with

$$m=\tfrac{1}{2} \quad \text{for } |\alpha|=\tfrac{1}{2};\tfrac{11}{2};\tfrac{13}{2}, \tag{34}$$

$$m=\tfrac{3}{2} \quad \text{for } |\alpha|=\tfrac{3}{2};\tfrac{9}{2};\tfrac{15}{2}, \tag{35}$$

$$m=\tfrac{5}{2} \quad \text{for } |\alpha|=\tfrac{5}{2};\tfrac{7}{2};\tfrac{17}{2}. \tag{36}$$

We emphasize that (for simplicity) the relations displayed here apply only to the case $\Gamma=6$, i.e., the first BZ is described by six wave vectors. All numerical work described in later sections employed the finer net size, $\Gamma=14$. The analogous relations for this case are easily found.

Compared with Eq. (27), the wave functions (32) have less variational freedom, as the coefficients $a_\alpha, b_\alpha, c_\alpha, d_\alpha, f_\alpha$ (determined by diagonalizing the Hamiltonian matrix) are now not independent variational parameters but functions of the first- and second-harmonic potentials G_m and H_m, which are two of the variational parameters (for each m).

The wave function of nuclear matter built with Bloch functions, normalized in a box of volume LD^2, is a single Slater determinant of one-particle states

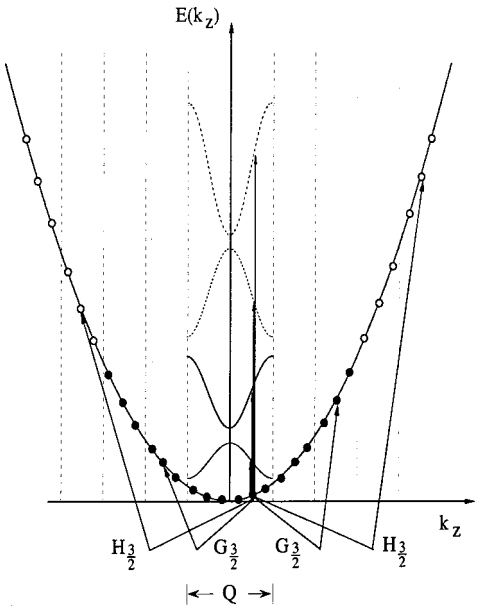

FIG. 7. The extended- and reduced-zone schemes for the nearly free-nucleon model with the first three BZ's fully occupied (full dots) and the rest of the states empty (empty dots). The periodic mixing potential connects states that differ by $\pm Q$ and $\pm 2Q$ as shown with arrows for the state $m=3/2$ for both the extended- and reduced-zone schemes. This potential opens up energy gaps at BZ boundaries, shown by the vertical dashed lines.

$$\psi_{\mathbf{k}_\perp,\alpha}(\boldsymbol{\rho},z)=\frac{1}{D}e^{\imath\mathbf{k}_\perp\cdot\boldsymbol{\rho}}\varphi_\alpha(z). \tag{37}$$

It is convenient to introduce fractional occupancies of each mode, A_α, defined by

$$A_\alpha\equiv\frac{N_\alpha}{A}, \tag{38}$$

where A is the total number of nucleons in the volume LD^2, and, since $A_\alpha=A_{-\alpha}$, N_α is the total number of nucleons in mode α and $-\alpha$. We can take the normalization condition (for three occupied bands) to be

$$\sum_{\alpha=1/2}^{17/2}A_\alpha=1. \tag{39}$$

The expression for the binding energy of the system is derived as follows. The kinetic energy can be divided into the (x, y) plane and z components. The average value for the (x, y)-plane component is that for any two-dimensional degenerate Fermi gas:

$$\langle k_\perp^2\rangle=\sum_{\alpha=1/2}^{17/2}A_\alpha\langle k_{\perp_\alpha}^2\rangle, \tag{40}$$

$$\langle k_{\perp_\alpha}^2\rangle=\frac{1}{2}\left(\frac{\pi}{D^2}\frac{N_\alpha}{\sigma}\right), \tag{41}$$

where σ is the total number of Bloch states (out of the 1-D continuum) that have been assigned to mode α and $-\alpha$, i.e., the number of states in the FBZ divided by $(1/2)\Gamma$,

$$\sigma=2\left(\frac{QL}{2\pi\Gamma}\right). \tag{42}$$

The factor 2 is required because A_α in Eq. (39) includes the nucleons from both α and $-\alpha$. [Equation (41) includes both spin and isospin degeneracy.] Upon introducing the average nucleon density (in the volume LD^2),

$$\rho_B\equiv\frac{A}{LD^2}, \tag{43}$$

one finds from Eqs. (41) and (42),

$$\langle k_{\perp_\alpha}^2\rangle=\pi^2\rho_B A_\alpha\left(\frac{\Gamma}{2Q}\right), \tag{44}$$

so that,

$$\langle k_\perp^2\rangle=\pi^2\rho_B\left(\frac{\Gamma}{2Q}\right)\sum_{\alpha=1/2}^{17/2}A_\alpha^2. \tag{45}$$

The z component of kinetic energy can be obtained from Eq. (32):

$$\begin{aligned}\langle k_z^2\rangle&=\sum_{\alpha=1/2}^{17/2}A_\alpha k_{z_\alpha}^2\\&=\left(\frac{Q}{\Gamma}\right)^2\sum_\alpha A_\alpha\{\alpha_\alpha^2(m-2\Gamma)^2\\&\quad+b_\alpha^2(m-\Gamma)^2+c_\alpha^2m^2+d_\alpha^2(m+\Gamma)^2+f_\alpha^2(m+2\Gamma)^2\\&\quad+\tfrac{1}{12}\},\end{aligned} \tag{46}$$

with the help of Eqs. (32)–(36). The additional term 1/12 in the sum represents the correction obtained by comparing the integral of k_z^2 from $-1/2Q$ to $1/2Q$ with the sum of the Γ discrete values, $k_{z_\alpha}^2$. The average total kinetic energy per nucleon is, of course, the sum of Eqs. (45) and (46).

$$\langle T\rangle=\frac{\hbar^2}{2\mu}(\langle k_\perp^2\rangle+\langle k_z^2\rangle). \tag{47}$$

The wave functions (32) must be used to compute the nucleon density,

$$\begin{aligned}\rho&=\sum_{\alpha=-17/2}^{17/2}N_\alpha|\psi_{\mathbf{k}_\perp,\alpha}(\boldsymbol{\rho},z)|^2=A\sum_{\alpha=1/2}^{17/2}A_\alpha|\psi_{\mathbf{k}\perp,\alpha}(\boldsymbol{\rho},z)|^2\\&=\rho_B\sum_{n=0}^{4}g_n\cos(nQz),\end{aligned} \tag{48}$$

with

$$g_0=\sum_{\alpha=1/2}^{17/2}A_\alpha K_\alpha(a_\alpha^2+b_\alpha^2+c_\alpha^2+d_\alpha^2+f_\alpha^2)\equiv 1, \tag{49}$$

$$g_1 = 2\sum_{\alpha=1/2}^{17/2} A_\alpha K_\alpha (a_\alpha b_\alpha + b_\alpha c_\alpha + c_\alpha d_\alpha + d_\alpha f_\alpha), \tag{50}$$

$$g_2 = 2\sum_{\alpha=1/2}^{17/2} A_\alpha K_\alpha (a_\alpha c_\alpha + b_\alpha d_\alpha + c_\alpha f_\alpha), \tag{51}$$

$$g_3 = 2\sum_{\alpha=1/2}^{17/2} A_\alpha K_\alpha (a_\alpha d_\alpha + b_\alpha f_\alpha), \tag{52}$$

$$g_4 = 2\sum_{\alpha=1/2}^{17/2} A_\alpha K_\alpha a_\alpha f_\alpha . \tag{53}$$

The number of Fourier components in the density depends on the dimension of the Hamiltonian matrix. For the case we have been considering, $\Gamma = 6$ and a 5×5 Hamiltonian, each state is mixed with four other states, $k_z \pm Q$ and $k_z \pm 2Q$. Equation (48) then exhibits four (nontrivial) density components: g_1, g_2, g_3, and g_4. In Sec. V, where we consider a 15×15 Hamiltonian, we find 14 density harmonics.

The potential (6) is employed to calculate the interaction energy,

$$V^\alpha = -\tfrac{1}{2}\alpha C[1 - g_\alpha(\langle T\rangle)] \int \rho(\mathbf{r}_1)\rho(\mathbf{r}_2)(\mathbf{r}_1 - \mathbf{r}_2)^2 \times \exp[(\mathbf{r}_1 - \mathbf{r}_2)^2/s^2] d^3\mathbf{r}_1 d^3\mathbf{r}_2, \tag{54}$$

which is the attractive energy; and

$$V^\beta = \tfrac{1}{2}\beta\sqrt{\langle T\rangle} \int \rho(\mathbf{r}_1)\rho(\mathbf{r}_2)\delta(\mathbf{r}_1 - \mathbf{r}_2) d^3\mathbf{r}_1 d^3\mathbf{r}_2, \tag{55}$$

which is the repulsive energy. Substituting Eq. (48) for the density, and observing that only the same harmonics in integrals of Eqs. (54) and (55) survive, we find expressions for the attractive and repulsive energies (per nucleon),

$$\langle V^\alpha\rangle \equiv \frac{V^\alpha}{A} = -\tfrac{1}{2}\alpha\rho_B[1 - g_s(\langle T\rangle)] \times \left\{ 1 + \frac{1}{2}\sum_{n=1}^{4} g_n^2 [1 - \tfrac{1}{6}(snQ)^2] e^{-1/4(snQ)^2} \right\}, \tag{56}$$

and

$$\langle V^\beta\rangle \equiv \frac{V^\beta}{A} = \tfrac{3}{8}\beta\sqrt{\langle T\rangle}\rho_B \left(1 + \frac{1}{2}\sum_{n=1}^{4} g_n^2 \right). \tag{57}$$

Finally, the total energy per nucleon is

$$-B = \langle T\rangle + \langle V^\alpha\rangle + \langle V^\beta\rangle. \tag{58}$$

The energy functional B for the case considered here ($\Gamma = 6$ and three energy bands occupied) depends on 16 independent variables [after recognizing the constraint (39)]:

$$B = B(\rho_B, Q; A_{3/2}, A_{5/2}, \ldots, A_{17/2}; G_{1/2}, G_{3/2}, G_{5/2}, H_{1/2}, H_{3/2}, H_{3/2}). \tag{59}$$

In general, if the first M energy bands are occupied, the number of independent variational parameters in B is

$$2 + (M \times \tfrac{1}{2}\Gamma - 1) + 2 \times \tfrac{1}{2}\Gamma = \Gamma(1 + \tfrac{1}{2}M) + 1.$$

Throughout the study that follows, we use $\Gamma = 14$. Thus the number of independent parameters for the case of M filled energy bands is

$$7M + 15. \tag{60}$$

Therefore, for $M = 10$, the maximum number of occupied bands considered, there are 85 variational parameters.

If, upon minimization, the optimum values of G_m and H_m differ from zero, the nuclear matter exhibits a broken translational symmetry. Occurrence of such an NDW is indeed found in Sec. V.

IV. VARIATIONAL PROCEDURE

The minimization procedure begins with assumed starting values for all $(7M + 15)$ variables, v_i, and initial increments, δv_i. (M is the number of occupied energy bands.) Each v_i in turn is changed to $v_i + \delta v_i$, and B is recomputed. If B is increased, the new value is kept. If B is decreased, v_i is changed to $v_i + 1/2\,\delta v_i$; the sign of the (subsequent) increment is then reversed and its magnitude reduced by half. Special care is required when incrementing $\{A_i\}$ on account of the constraint, Eq. (39). This requirement is easily achieved: when A_i is changed to $A_i + \delta A_i$, all $\{A_j\}$ are then divided by $1 + \delta A_i$. (Since all A_i must remain positive, A_i is set to zero if it becomes negative; the subsequent increment is reduced by half and is positive.)

The program was first tested by setting all G_m and H_m to zero. The initial Q was taken to be $2k_F/M$. In less then 100 iterations, involving $(7M + 1)$ variables, B converged to $B_0 (= 15\,\text{MeV/nucleon})$, and $\{A_\alpha\}$ converged to values expected for a Fermi sphere. If the 14 coupling potentials $\{G_m, H_m\}$ were allowed to deviate incrementally from zero, B converged to B_0 and $\{G_m, H_m\}$ converged back to zero. The HF solution for uniform nuclear matter is therefore a robust metastable state. [Unless initial parameters already describe a significant NDW modulation, the iterative procedure returns to the uniform solution. Indeed one must incorporate at the onset the discontinuities in $k_F(k_z)$ at the Brillouin-zone energy gaps, as shown in Fig. 8; otherwise the instability does not arise.]

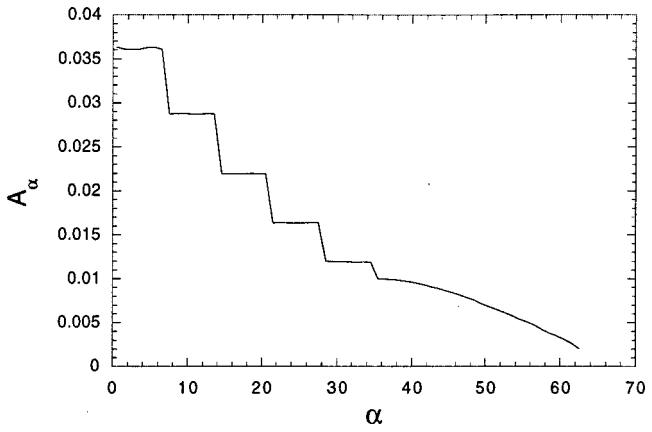

FIG. 8. The fractional occupancies A_α for $M=9(15\times15)$. $\alpha=\Gamma k_z/Q$, $(\Gamma=14)$.

The global maximum for B was found by iterating all $(7M+15)$ variables with starting G's and H's corresponding to 10 and 4 MeV, respectively. The starting $\{A_\alpha\}$ were taken to be constant in each energy band j but with a common difference, A_j-A_{j-1}, between (adjacent) bands. We found (by trial and error) that this prescription always produces convergence to the global maximum after 550 iterations. (Starting increments were typically 1–5 % of expected final values.)

V. NDW IN NUCLEAR MATTER, RESULTS

The HF ground state of symmetric nuclear matter is obtained by optimizing the energy functional, e.g., Eq. (59), with respect to all $(7M+15)$ independent variables. As mentioned above, in our calculations the size of the mixing Hamiltonian varied from 9×9 to 15×15. Even though the number of variational parameters remains the same, the larger dimension of the Hamiltonian matrix allows greater variational freedom for the Bloch functions because more momentum space is probed. The larger matrices introduce extra density harmonics in Eq. (48) and always lead to an increase in binding energy per nucleon. A discrete parameter at our disposal is the allowed number of occupied Brillouin zones, M. A larger M corresponds to a smaller Q since $Q\sim2k_F/M$.

The results of our variational calculations are presented in Fig. 9. The binding energy per nucleon in the absence of an NDW is 15 MeV in all cases. On introducing nonzero G's and H's the optimum B first exceeds 15 MeV at $M=5$ ($Q=0.42\,\mathrm{fm}^{-1}$). Then, depending on the size of the Hamiltonian, the excess binding saturates at $M=6$ for 9×9, $M=7$ for 11×11, $M=8$ for 13×13, and $M=9$ for 15×15. Saturation in binding occurs when the extra band, included in the variational scheme, nevertheless remains unoccupied. For example, the $M=7(9\times9)$ configuration has essentially no nucleons in the seventh band; the distribution of nucleons in the first six bands is virtually identical to that obtained for the $M=6(9\times9)$ configuration.

The extra binding caused by the NDW for $M=9(15\times15)$ is $\Delta B=1.51$ MeV/nucleon. The energy functional in this case has 78 variables. Their final values are

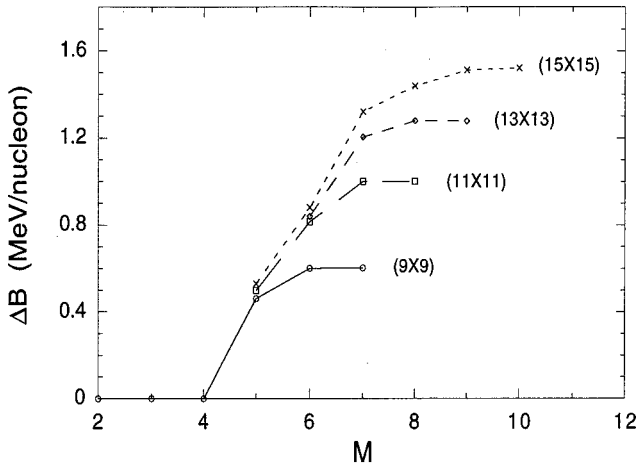

FIG. 9. The extra binding energy per nucleon (relative to $B_0=15$ MeV) caused by an NDW in nuclear matter vs the number M of allowed occupied bands.

$$\rho_B=0.116\ \ \mathrm{fm}^{-3},$$

$$Q=0.234\ \ \mathrm{fm}^{-1},$$

$$G_{1/2}=G_{3/2}=\cdots=G_{13/2}=10.2\mathrm{MeV}/(\hbar^2/2\mu),$$

$$H_{1/2}=H_{3/2}=H_{7/2}=3.8\ \ \mathrm{MeV}/(\hbar^2/2\mu),$$

$$H_{5/2}=H_{9/2}=H_{11/2}=H_{13/2}=4.0\ \ \mathrm{MeV}/(\hbar^2/2\mu).$$

The distribution of the 63 fractional occupancies, A_α, is shown in Fig. 8. The fractional occupancy determines the Fermi radius of the 2-D nucleon gas for each k_{z_α}:

$$k^{\perp}_{F_\alpha}=\pi\sqrt{\rho_B A_\alpha\Gamma/Q}.$$

The Fermi surface is shown in Fig. 10. The discontinuities are caused by the energy gaps at the BZ boundaries. The amplitudes of the density harmonics are

$$g_1=1.032,\quad g_2=0.454,\quad g_3=6.171\times10^{-2},$$

$$g_4=-1.255\times10^{-4},$$

$$g_5=-4.254\times10^{-3},\quad g_6=-1.412\times10^{-4},$$

$$g_7=-4.538\times10^{-4},\quad g_8=-4.064\times10^{-4},$$

$$g_9=-1.782\times10^{-4},\quad g_{10}=-1.727\times10^{-4},$$

$$g_{11}=-1.263\times10^{-4},$$

$$g_{12}=-6.603\times10^{-5},\quad g_{13}=-2.243\times10^{-5},$$

$$g_{14}=-4.456\times10^{-6}.$$

The solution for $M=10(15\times15)$ is the same as that for $M=9$, since the tenth band remains unoccupied.

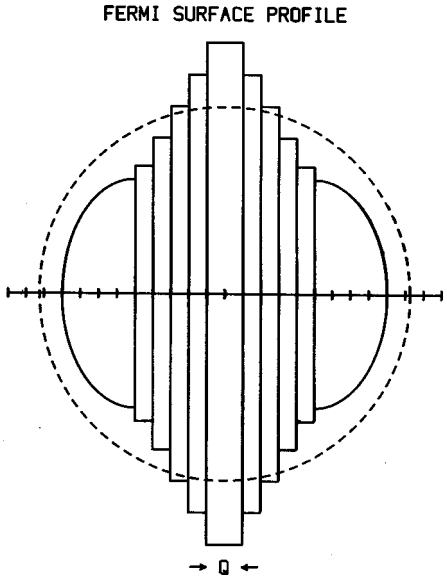

FIG. 10. The 3-D Fermi surface corresponding to Fig. 9. The horizontal line is the axis of symmetry. The dashed sphere is the Fermi sphere of equal volume.

The nucleon density profile along the intrinsic axis is shown in Fig. 11. The NDW has a large peak-to-trough ratio of ~ 7. The wavelength is, $a = 26.9$ fm. The profile is dominated by the first and second harmonics, as can be seen from Fig. 11. Apart from increasing the density at the peaks, and thus facilitating the instability, the large second harmonic is necessary to prevent the density from going negative. The average nucleon density is smaller than that for uniform nuclear matter.

Also shown in Fig. 11 is the density profile of a Gaussian slab (modality 7). The NDW solution is similar to a periodic array of Gaussian slabs. The nuclear density that forms a bridge between adjacent slabs increases the binding energy by ~ 0.6 MeV/nucleon compared to that for an isolated Gaussian slab.

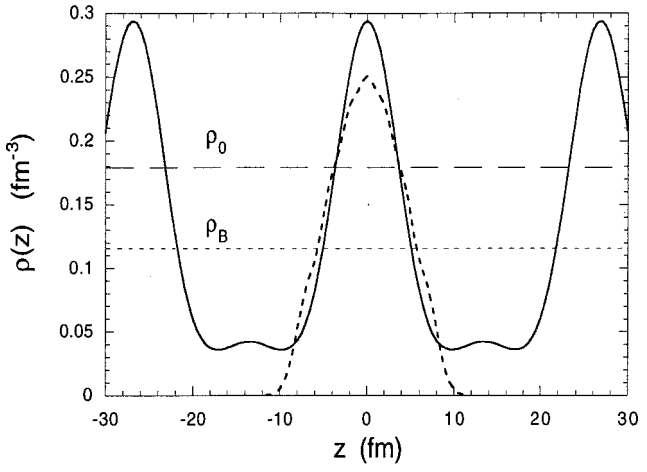

FIG. 11. The nucleon density profile along the z axis for $M = 9(15\times 15)$ (solid line) and the density profile of a Gaussian slab (modality 7) of nuclear matter (thick dashed line). The two horizontal lines indicate the equilibrium density of uniform nuclear matter (long-dash line), and the average nucleon density for the NDW (short-dash line).

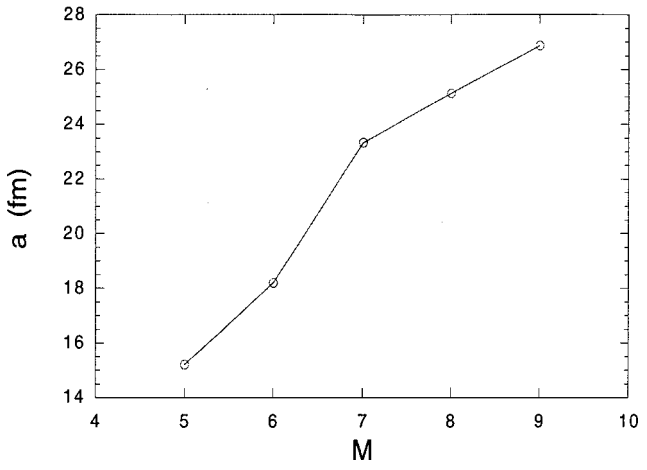

FIG. 12. The wavelength of an NDW vs the number M of occupied energy bands. [All points correspond to a (15×15) mixing Hamiltonian.]

The wavelength a of an NDW depends on the number M of occupied Bloch bands, as shown in Fig. 12. This result is expected at the outset since $Q \approx 2k_F/M$ and $a = 2\pi/Q$. A stable NDW first occurs for $M = 5$. The corresponding density profile is shown in Fig. 13. The peak-to-trough ratio is ~ 6. The effective mixing potentials are

$$G_m = 9.3 \text{ MeV}/(\hbar^2/2\mu) \text{ and } H_m = 2.1\text{MeV}/(\hbar^2/2\mu).$$

The wavelength is $a = 15.2$ fm.

VI. DISCUSSION

The results of the previous section show that the HF ground state of symmetric nuclear matter has a broken translational symmetry, namely, one (or more) NDW's. Whether there is more than one is a subject for future research. An

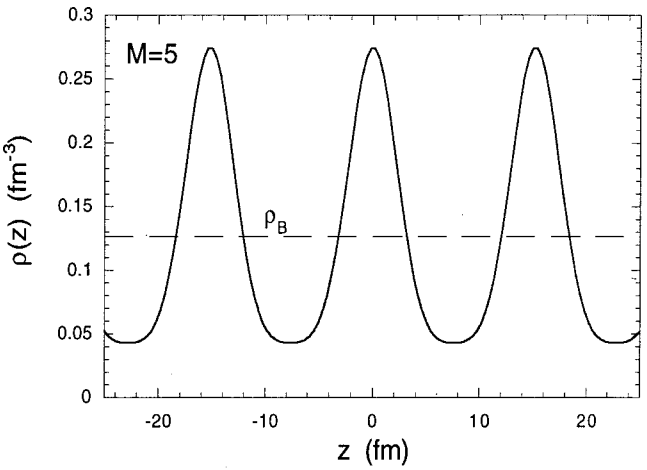

FIG. 13. The nucleon density profile along the z axis for $M = 5(15\times 15)$. The average nucleon density is shown by the dashed line.

NDW arises when a periodic self-consistent potential mixes orbitals having a wave-vector component k_z with $k_z \pm Q$, $(Q < 2k_F/5)$. The wavelength a of the instability (inversely proportional to Q) can vary from 15 to 27 fm. The NDW is strongly modulated with a peak-to-trough ratio of 6 to 7. The lower average density, $\rho_B \sim 0.65-0.71\rho_0$, is a likely result of the higher kinetic pressure caused by the kinetic energy increase associated with the modulation. This increase, however, is offset by a larger increase in attractive energy. The net result is an extra 0.5–1.5 MeV/nucleon of binding energy (compared with that of uniform nuclear matter). It is important to emphasize the collective nature of the instability. It probably could not be discovered in a routine HF procedure. (Uniform nuclear matter is a robust metastable state.)

A possible application of the method developed here is to neutron-star matter. The search for new phases of dense nuclear matter but, on average, below saturation density may benefit from our finding that the uniform nucleon (vapor) phase and, possibly, the bubble phase (nucleon vapor filling cavities in dense nuclear matter) are highly excited states relative to an NDW. Other (nonspherical) geometries for nuclear matter may result within the Bloch-function framework developed here.

Another possible application is the search for an island of stability in superheavy elements. We can entertain the idea of performing calculations similar to those completed here but with localized wave functions in the (x, y) plane. Instead of plane waves, one might take basis functions from a two-dimensional harmonic oscillator. Bloch functions, introduced here, would be retained for the z direction. The infinite nucleon system would then resemble a chain of beads.

A superdeformed heavy nucleus might resemble two beads linked together. The density profile along the intrinsic axis can be imagined from Fig. 13, but terminated at $z = -20$ and $z = 5$ fm. It would be very interesting to compare the potential barrier against spontaneous fission (calculated in this way) to the current estimates derived from shell-model-type calculations [3]. A shape excitation from two beads (one trough) to three beads (two troughs) might describe fission isomerism as well as the dichotomy of symmetric and asymmetric fission.

The insight that supports the foregoing suggestions stems from Sec. II, where we found that symmetric (charge-free) nuclear matter of optimum density is unstable for fission into isolated nucleon slabs having a thickness of ~ 12 fm. This result implies that the surface energy for each face of a slab is ~ -1 MeV/fm^2, instead of ~ 1.1 MeV/fm^2, a value based on the surface term of the semiempirical mass formula. Although a surface energy that depends on surface curvature has been entertained from time to time, we are unaware of any prior suggestion that it might in fact change sign.

A negative surface energy seems counterintuitive at first sight. Indeed, such would be the case if the nucleon density (of a semi-infinite system) were to fall monotonically to zero from its interior value, ρ_0. However, monotonic behavior does not occur, even for a noninteracting Fermi gas, near a boundary where $\rho(z)$ must be zero. As z approaches the surface (say at $z = 0$), $\rho(z)$ rises to a peak before it falls to zero [4]. Attractive nucleon-nucleon interactions will cause such a peak to be enhanced. Consequently the extra binding energy generated in the peak can more than compensate for the loss that occurs when $\rho(z) < \rho_0$. The $\rho(z)$ profiles of Figs. 4 and 5 illustrate this phenomenon. Clearly, the fall in surface energy, especially a change in sign, can occur only in very heavy, or superheavy nuclei where opposite surfaces are ~ 12 fm apart. Unexpected stability of fissionable or superheavy species may result.

VII. CONCLUSIONS

This study shows that symmetric (three-dimensional) nuclear matter exhibits a spontaneously broken translational symmetry. This collective instability creates a one-dimensional nucleon density wave of periodicity 15–27 fm, with a peak-to-trough density ratio of ~ 6. A result of the instability is that the binding energy of the system is increased by 0.5–1.5 MeV per nucleon relative to that for uniform nuclear matter, which must now be considered a highly excited metastable state.

Such collective instabilities may be important in the search for an island of stability in superheavy nuclei and to new understanding of the mechanism of fission.

The validity of the foregoing conclusions may be judged in light of the following considerations. In formulating [2] the three-parameter potential, Eq. (6), we always chose (when there was an option) the alternative that was least favorable for generating a broken symmetry. In other words, we ''stacked the deck'' against the possible occurrence of an NDW by underestimating the strength of the instability in the following ways. [This strength depends primarily on the magnitude of the Fourier component of $V(r)$ at $q = Q$, i.e., on $V(q = Q)$.]

(1) An attractive Gaussian instead of $r^2 \times$Gaussian would have been more convenient. However, we adopted the latter in order to obtain a better fit to the binding energy of ^{16}O. The Fourier transform of the latter potential falls off faster than that for a simple Gaussian. Consequently, $V(q = Q)$ is smaller (in magnitude) and the NDW instability is weaker.

(2) A finite-range repulsion is, of course, more realistic than a δ function. Had we employed such a repulsion, its Fourier transform would fall off with q, in contrast to that of a δ function (which does not). Consequently, $V(q = Q)$ would be larger (in magnitude) because there would be less cancellation of the attractive contribution. By retaining the δ function repulsive core, we have again underestimated the NDW instability.

(3) The nucleon effective mass, $m^* = 0.41m$, for the effective interaction derived in Ref. [2] is somewhat smaller than values, 0.6–0.8, found by other workers. Had we fiddled with the repulsion to bring m^* up to, say 0.6, the NDW instability would be even more robust. The reason is that the excitation energy to convert pure plane waves to Bloch functions and the repopulation energy to change a Fermi sphere into the faceted shape shown in Fig. 10 are both inversely proportional to m^*. A larger m^* reduces the energy increase that needs to be compensated by the attractive term.

(4) The uniform-density state is described by a Slater de-

terminant of pure plane waves. This wave function is an exact solution of the Hartree-Fock scheme. Its energy cannot be lowered by any of an infinite number of small modifications. In contrast, the shape of each Bloch function depends on only two parameters, $G(k)$ and $H(k)$, in the off-diagonal lines of the matrix following Eq. (27). We could have included up to 12 additional off-diagonal lines (for a 15×15 matrix). Each additional parameter, $J(k)$, $L(k)$, $M(k)$, etc. would lead incrementally to an even lower energy for the NDW phase. Since the NDW instability is 1.5 MeV/nucleon when using only two parameters, there is no need to embellish the demonstration of the NDW phase with extra (energetically favorable) complications.

Even though we have shown that the variational (Hartree-Fock) state for an NDW has lower energy than the (exact) Hartree-Fock state with uniform density, one may inquire about many-body corrections beyond the Hartree-Fock scheme. Such an investigation [5] indicates that density-wave modulations enhance the matrix elements for virtual scattering and so increase the magnitude of the (negative) correlation energy. Since the ''correct'' nucleon-nucleon interaction in nuclear matter is unknown, and since the many-body problem is insoluable, the usual caveat applies here as elsewhere.

Nevertheless, we believe that any effective interaction that reproduces the binding energy, saturation density, compressibility modulus, and effective mass in nuclear matter, and is also consistent with the surface energy of light nuclei, e.g., ^{4}He, ^{16}O, ^{40}Ca, will also exhibit the collective instabilities we have found using our potential, Eq. (6), which fulfills these seven requisites. This broken translational symmetry is not revealed by small variational excursions near uniform nuclear matter, which is instead a robust (but metastable) highly excited state.

APPENDIX: BINDING ENERGY IN A SLAB OF SYMMETRIC NUCLEAR MATTER

We begin with the one-particle nucleon wave functions of Eq. (13):

$$\psi^0_{\mathbf{k},m}(\boldsymbol{\rho},z)=Ne^{i\mathbf{k}\cdot\boldsymbol{\rho}}\varphi_m(z). \tag{A1}$$

With the notation, $\eta\equiv\mu\omega/\hbar$, $\mu\equiv1/2(m_p+m_n)$, the first seven normalized one-dimensional oscillator wave functions are

$$\varphi_0(z)=\left(\frac{\eta}{\pi}\right)^{1/4}e^{-1/2\,\eta z^2}$$

$$\varphi_1(z)=\left(\frac{\eta}{\pi}\right)^{1/4}\sqrt{2\,\eta}z\,e^{-1/2\,\eta z^2}$$

$$\varphi_2(z)=\left(\frac{\eta}{\pi}\right)^{1/4}\frac{1}{\sqrt{2}}(2\,\eta z^2-1)e^{-1/2\,\eta z^2}$$

$$\varphi_3(z)=\left(\frac{\eta}{\pi}\right)^{1/4}\frac{1}{\sqrt{3}}(2\,\eta^{3/2}z^3-3\,\eta^{1/2}z)e^{-1/2\,\eta z^2}$$

$$\varphi_4(z)=\left(\frac{\eta}{\pi}\right)^{1/4}\frac{1}{\sqrt{24}}(4\,\eta^2z^4-12\,\eta z^2+3)e^{-1/2\,\eta z^2}$$

$$\varphi_5(z)=\left(\frac{\eta}{\pi}\right)^{1/4}\frac{1}{\sqrt{60}}(4\,\eta^{5/2}z^5-20\,\eta^{3/2}z^3+15\,\eta^{1/2}z)e^{-1/2\,\eta z^2}$$

$$\varphi_6(z)=\left(\frac{\eta}{\pi}\right)^{1/4}\frac{1}{\sqrt{720}}(8\,\eta^3z^6-60\,\eta^2z^4+90\,\eta z^2-15)\times e^{-1/2\,\eta z^2}.$$

In a slab of modality $M+1$ $(m=0,1,...,M)$ we introduce wave-function mixing between two modes, m and $m'=m+2$, according to the following scheme. For $m=0,1,...,M-2$,

$$\psi^0_{\mathbf{k},m}\rightarrow\psi_{\mathbf{k},m}$$

$$=\begin{cases}\psi^0_{\mathbf{k},m}\equiv|m\rangle, & \text{if } k_m\leqslant k_{F_{m+2}}\\ \dfrac{1}{\sqrt{1+c_m^2}}(\psi^0_{k,m}+c_m\psi^0_{k,m+2})\equiv|m^*\rangle, & \text{if } k_m>k_{F_{m+2}}.\end{cases} \tag{A2}$$

For $m=M-1$ and M,

$$\psi^0_{\mathbf{k},m}\rightarrow\psi_{\mathbf{k},m}=\frac{1}{\sqrt{1+c_m^2}}(\psi^0_{\mathbf{k},m}+c_m\psi^0_{\mathbf{k},m+2})$$
$$=|m^*\rangle \quad \text{for any } k_m. \tag{A3}$$

The last two occupied modes, $M-1$ and M, are treated differently because they are mixed with completely empty modes, $M+1$ and $M+2$, while the first $M-1$ modes are mixed with partially occupied modes 2,3,...,M. The mixing-strength coefficients c_m are independent variables in the variational Hartree-Fock procedure.

We define a density parameter,

$$\rho_G\equiv\frac{A}{L^2\sqrt{2\,\pi/\eta}}, \tag{A4}$$

where A is the total number of nucleons and L^2 is the area of each surface of the slab. The two-dimensional Fermi sea corresponding to each mode m is a disk of area

$$\pi k^2_{F_m}=\pi^2\frac{A_mA}{L^2}=\pi^2\left(\frac{2\,\pi}{\eta}\right)^{1/2}A_m\rho_G. \tag{A5}$$

A_m is the fractional occupancy of the mth mode (so that the number of nucleons in the mth mode is $N_m=A_mA$). In the mixing scheme of Eq. (A2) and (A3), the number of states in the mth mode that undergo mixing with the $(m+2)$th mode is proportional to the difference in areas of the mth and $(m+2)$th Fermi disks.

Consider a generic real two-particle operator U. We want to calculate its expectation value $U_{mm'}$ for two nucleons in two different oscillator modes, m and m', $(m<m')$. We have to distinguish three situations:

(1) $m' \leqslant M-2$. The four mixing possibilities in this case are

$$\text{(a)} \quad k_m \leqslant k_{F_{m+2}} \text{ and } k_{m'} \leqslant k_{F_{m'+2}},$$

$$\text{(b)} \quad k_m \leqslant k_{F_{m+2}} \text{ and } k_{m'} > k_{F_{m'+2}},$$

$$\text{(c)} \quad k_m > k_{F_{m+2}} \text{ and } k_{m'} \leqslant k_{F_{m'+2}},$$

$$\text{(d)} \quad k_m > k_{F_{m+2}} \text{ and } k_{m'} > k_{F_{m'+2}}.$$

The relative weights of these possibilities are

$$\text{(a)} \quad \frac{k^2_{F_{m+2}}}{k^2_{F_m}} \times \frac{k^2_{F_{m'+2}}}{k^2_{F_{m'}}} = \frac{A_{m+2}A_{m'+2}}{A_m A_{m'}},$$

$$\text{(b)} \quad \frac{k^2_{F_{m+2}}}{k^2_{F_m}} \times \left(1 - \frac{k^2_{F_{m'+2}}}{k^2_{F_{m'}}}\right) = \frac{A_{m+2}}{A_m}\left(1 - \frac{A_{m'+2}}{A_{m'}}\right),$$

$$\text{(c)} \quad \left(1 - \frac{k^2_{F_{m+2}}}{k^2_{F_m}}\right) \times \frac{k^2_{F_{m'+2}}}{k^2_{F_{m'}}} = \left(1 - \frac{A_{m+2}}{A_m}\right)\frac{A_{m'+2}}{A_{m'}},$$

$$\text{(d)} \quad \left(1 - \frac{k^2_{F_{m+2}}}{k^2_{F_m}}\right) \times \left(1 - \frac{k^2_{F_{m'+2}}}{k^2_{F_{m'}}}\right) = \left(1 - \frac{A_{m+2}}{A_m}\right)\left(1 - \frac{A_{m'+2}}{A_{m'}}\right).$$

(2) $m \leqslant M-2$, $m' > M-2$. The two possibilities are

$$\text{(a)} \quad k_m \leqslant k_{F_{m+2}}, \text{ for all } k_{m'},$$

$$\text{(b)} \quad k_m > k_{F_{m+2}}, \text{ for all } k_{m'},$$

with relative weights

$$(1) \quad \frac{k^2_{F_{m+2}}}{k^2_{F_m}} = \frac{A_{m+2}}{A_m},$$

$$(2) \quad \left(1 - \frac{k^2_{F_{m+2}}}{k^2_{F_m}}\right) = \left(1 - \frac{A_{m+2}}{A_m}\right).$$

(3) $m > M-2$, $m' > M-2$. In this case mixing occurs independent of the size of k_m and $k_{m'}$.

The expectation value $U_{mm'}$ in these three cases is

$$(1) \quad U_{mm'} = \frac{A_{m+2}A_{m'+2}}{A_m A_{m'}} U^{oo}_{mm'} + \frac{A_{m+2}}{A_m}\left(1 - \frac{A_{m'+2}}{A_{m'}}\right) U^{o*}_{mm'} + \left(1 - \frac{A_{m+2}}{A_m}\right)\frac{A_{m'+2}}{A_{m'}} U^{*o}_{mm'} + \left(1 - \frac{A_{m+2}}{A_m}\right) \times \left(1 - \frac{A_{m'+2}}{A_{m'}}\right) U^{**}_{mm'}, \tag{A6}$$

$$(2) \quad U_{mm'} = \frac{A_{m+2}}{A_m} U^{oo}_{mm'} + \left(1 - \frac{A_{m+2}}{A_m}\right) U^{*o}_{mm'}, \tag{A7}$$

$$(3) \quad U_{mm'} = U^{oo}_{mm'}, \tag{A8}$$

where, in the notation of Eq. (A2) and (A3),

$$U^{oo}_{mm'} \equiv \langle m, m' | U | m, m' \rangle, \tag{A9}$$

$$U^{o*}_{mm'} \equiv \langle m, m'* | U | m, m'* \rangle = \frac{1}{1+c^2_{m'}} (\langle m, m' | U | m, m' \rangle + 2c_{m'} \langle m, m' + 2 | U | m, m' \rangle + c^2_{m'} \langle m, m'+2 | U | m, m'+2 \rangle), \tag{A10}$$

$$U^{*o}_{mm'} \equiv \langle m*, m' | U | m*, m' \rangle = \frac{1}{1+c^2_m} (\langle m, m' | U | m, m' \rangle + 2c_m \langle m+2, m' | U | m, m' \rangle + c^2_m \langle m+2, m' | U | m+2, m' \rangle), \tag{A11}$$

$$U^{**}_{mm'} \equiv \langle m*, m'* | U | m*, m'* \rangle = \frac{1}{(1+c^2_m)(1+c^2_{m'})} (\langle m, m' | U | m, m' \rangle + 2c_m \langle m+2, m' | U | m, m' \rangle + c^2_m \langle m+2, m' | U | m+2, m' \rangle + 2c_{m'} \langle m, m'+2 | U | m, m' \rangle + c^2_{m'} \langle m, m'+2 | U | m, m'+2 \rangle + 4c_m c_{m'} \langle m+2, m'+2 | U | m, m' \rangle + 2c_m c^2_{m'} \times \langle m+2, m'+2 | U | m, m'+2 \rangle + 2c_{m'} c^2_m \langle m+2, m'+2 | U | m+2, m' \rangle + c^2_m c^2_{m'} \langle m+2, m'+2 | U | m+2, m'+2 \rangle). \tag{A12}$$

For a one-particle real operator T its expectation value T_m is calculated in a similar way. Here the two distinct cases are (1) $m \leqslant M-2$. The two possibilities,

$$k_m \leqslant k_{F_{m+2}} \quad \text{and} \quad k_m > k_{F_{m+2}},$$

have relative probabilities

$$\frac{A_{m+2}}{A_m} \quad \text{and} \quad \left(1-\frac{A_{m+2}}{A_m}\right).$$

(2) $m=M-1,M$. In this case all the nucleons in the mth mode undergo mixing. The corresponding expectation values for the two cases are

$$\begin{aligned}(1)\quad T_m &= \frac{A_{m+2}}{A_m}\langle m|T|m\rangle + \left(1-\frac{A_{m+2}}{A_m}\right)\langle m^*|T|m^*\rangle \\ &= \frac{A_{m+2}}{A_m}\langle m|T|m\rangle + \left(1-\frac{A_{m+2}}{A_m}\right)\frac{1}{1+c_m^2}[\langle m|T|m\rangle \\ &\quad + c_m^2\langle m+2|T|m+2\rangle], \end{aligned} \tag{A13}$$

$$\begin{aligned}(2)\quad T_m &= \langle m^*|T|m^*\rangle \\ &= \frac{1}{1+c_m^2}[\langle m|T|m\rangle + c_m^2\langle m+2|T|m+2\rangle]. \end{aligned} \tag{A14}$$

Finally, if a two-particle operator U acts upon two states belonging to the same mode m, its expectation value for $m=0,...,M-2$ is

$$\begin{aligned}U_{mm} &= \frac{A_{m+2}}{A_m}\langle m,m|U|m,m\rangle + \left(1-\frac{A_{m+2}}{A_m}\right) \\ &\quad \times\langle m^*,m^*|U|m^*,m^*\rangle, \end{aligned} \tag{A15}$$

and for $m=M-1,M$,

$$U_{mm} = \langle m^*,m^*|U|m^*,m^*\rangle, \tag{A16}$$

with

$$\begin{aligned}&\langle m^*,m^*|U|m^*,m^*\rangle \\ &= \frac{1}{(1+c_m^2)^2}(\langle m,m|U|m,m\rangle + 4c_m\langle m+2,m|U|m,m\rangle \\ &\quad + 2c_m^2\langle m+2,m|U|m+2,m\rangle + 4c_m^2\langle m+2,m+2|U|m,m\rangle \\ &\quad + (4c_m^3\langle m+2,m+2|U|m+2,m\rangle \\ &\quad + c_m^4\langle m+2,m+2|U|m+2,m+2\rangle). \end{aligned} \tag{A17}$$

Now we can calculate the matrix elements of the kinetic energy operator and the nucleon-nucleon potential (6). Due to the separability of the (x, y) and z parts of the wave functions (A1), the average kinetic energy of a nucleon in the mth mode is

$$\begin{aligned}\langle T_m\rangle &= \frac{A_{m+2}}{A_m}\left\{\frac{\hbar^2}{2\mu}\langle k_m^2\rangle + \tfrac{1}{2}(m+\tfrac{1}{2})\hbar\omega\right\} + \left(1-\frac{A_{m+2}}{A_m}\right) \\ &\quad \times\frac{1}{1+c_m^2}\left\{(1+c_m^2)\frac{\hbar^2}{2\mu}\langle k_m^2\rangle + [\tfrac{1}{2}(m+\tfrac{1}{2}) \right. \\ &\quad \left. + \tfrac{1}{2}(m+2+\tfrac{1}{2})c_m^2]\hbar\omega\right\}, \end{aligned} \tag{A18}$$

for $m=0,...,M-2$; and

$$\begin{aligned}\langle T_m\rangle &= \frac{1}{1+c_m^2}\left\{(1+c_m^2)\frac{\hbar^2}{2\mu}\langle k_m^2\rangle + [\tfrac{1}{2}(m+\tfrac{1}{2}) \right. \\ &\quad \left. + \tfrac{1}{2}(m+2+\tfrac{1}{2})c_m^2]\hbar\omega\right\}, \end{aligned} \tag{A19}$$

for $m=M-1,M$. According to Eq. (A5), the average value of k_m^2 is

$$\langle k_m^2\rangle = \tfrac{1}{2}k_F^2 = \pi\left(\frac{\pi}{2\eta}\right)^{1/2}A_m\rho_G. \tag{A20}$$

Using $\omega\hbar=\hbar^2\eta/\mu$, the above equations may be rewritten as

$$\begin{aligned}\langle T_m\rangle &= \frac{\hbar^2}{2\mu}\left\{\pi\left(\frac{\pi}{2\eta}\right)^{1/2}A_m\rho_G + \frac{A_{m+2}}{A_m}(m+\tfrac{1}{2})\eta \right. \\ &\quad \left. + \left(1-\frac{A_{m+1}}{A_m}\right)\frac{1}{1+c_m^2}[(m+\tfrac{1}{2})+(m+\tfrac{5}{2})c_m^2]\eta\right\}, \end{aligned} \tag{A21}$$

for $m=1,...,M-2$; and

$$\langle T_m\rangle = \frac{\hbar^2}{2\mu}\left\{\pi\left(\frac{\pi}{2\eta}\right)^{1/2}A_m\rho_G + [(m+\tfrac{1}{2})+(m+\tfrac{5}{2})c_m^2]\eta\right\}, \tag{A22}$$

for $m=M-1,M$. The average kinetic energy per nucleon for the entire slab is

$$\langle T\rangle = \sum_{m=0}^{M} A_m\langle T_m\rangle. \tag{A23}$$

The average interaction energy per nucleon in the slab may be written as

$$\langle V\rangle = \tfrac{1}{2}A\sum_{m,m'}A_mA_{m'}([1-g_s(\langle T\rangle)]V_{mm'}^{\alpha} + \tfrac{3}{4}V_{mm'}^{\beta}), \tag{A24}$$

where the interaction potential (6) is broken up in two parts:

$$V^{\alpha} \equiv -\alpha C(\mathbf{r}-\mathbf{r}')^2 e^{(\mathbf{r}-\mathbf{r}')^2/s^2}, \tag{A25}$$

and

$$V^{\beta} \equiv \beta\sqrt{\langle T\rangle}\,\delta(\mathbf{r}-\mathbf{r}'). \tag{A26}$$

The factor, $[1-g_s(\langle T\rangle)]$, with

$$g_s(\langle T\rangle)=\frac{1}{2b^3\langle T\rangle^3}[-6+3b\langle T\rangle+3e^{-b\langle T\rangle}(2+b\langle T\rangle)], \tag{A27}$$

$$b\equiv\frac{10\mu s^2}{3\hbar^2}, \tag{A28}$$

appears as a statistical approximation to the HF exchange energy $V^{\alpha}_{\rm exch}$ (see [2] for details), and is replaced by the factor 3/4, exact result, for the zero-range repulsive term, V^{β}.

In order to evaluate matrix elements of the repulsive potential V^{α}, we separate variables in Eq. (A25) by letting

$$(\mathbf{r}-\mathbf{r}')^2=(\boldsymbol{\rho}-\boldsymbol{\rho}')^2+(z-z')^2. \tag{A29}$$

With new variables,

$$\mathbf{R}\equiv\boldsymbol{\rho}-\boldsymbol{\rho}', \tag{A30}$$

and

$$z\equiv Z+\tfrac{1}{2}\zeta, \quad z'\equiv Z-\tfrac{1}{2}\zeta, \tag{A31}$$

a generic matrix element, $\langle m,m'|V^{\alpha}|m'',m'''\rangle$, calculated with wave functions (A1) becomes

$$\begin{aligned}\langle m,m'|V^{\alpha}|m'',m'''\rangle&=\frac{\alpha C}{L^4}\int dz\,dz'\int d\boldsymbol{\rho}\,d\boldsymbol{\rho}'\,\varphi_m(z)\varphi_{m'}(z')\varphi_{m''}(z)\varphi_{m'''}(z')\\&\times[(\boldsymbol{\rho}-\boldsymbol{\rho}')^2+(z-z')^2]\exp[-(z-z')^2/s^2]\\&\times\exp[-(\boldsymbol{\rho}-\boldsymbol{\rho}')^2/s^2]\\&=\frac{\alpha C}{L^2}\int d\mathbf{R}[R^2e^{-R^2/s^2}I^{(1)}_{m,m',m'',m'''}\\&+e^{-R^2/s^2}I^{(2)}_{m,m',m'',m'''}]\\&=\frac{\alpha C}{L^2}\pi s^2[s^2I^{(1)}_{m,m',m'',m'''}+I^{(2)}_{m,m'',m'',m'''}],\end{aligned} \tag{A32}$$

where

$$I^{(1)}_{m,m',m'',m'''}(\eta,s)\equiv\int dZ\,d\zeta\,\varphi_m(Z,\zeta)\varphi_{m'}(Z,\zeta)\times\varphi_{m''}(Z,\zeta)\varphi_{m'''}(Z,\zeta)e^{-\zeta^2/s^2}, \tag{A33}$$

and

$$I^{(2)}_{m,m',m'',m'''}(\eta,s)\equiv\int dZ\,d\zeta\,\varphi_m(Z,\zeta)\varphi_{m'}(Z,\zeta)\times\varphi_{m''}(Z,\zeta)\varphi_{m'''}(Z,\zeta)\zeta^2e^{-\zeta^2/s^2}. \tag{A34}$$

The integrals (A33) and (A34) involve the Gaussians and the Hermite polynomials. They are readily calculated analytically (we used a procedure written in MAPLE language) and tabulated for all values $m,m',m'',m'''=0,1,...,M$. Having expressed the matrix element, $\langle m,m'|V^{\alpha}|m'',m'''\rangle$, as an analytic function of the parameter η, we use equations (A6)–(A12) and equations (A15)–(A17) to calculate the terms $V^{\alpha}_{m,m'}$ in equation (A24) and obtain the average attractive energy per nucleon in the slab $\langle V^{\alpha}\rangle$.

In a similar way, we calculate the matrix elements $\langle m,m'|V^{\beta}|m'',m'''\rangle$:

$$\begin{aligned}\langle m,m'|V^{\beta}|m'',m'''\rangle&=\frac{\beta\sqrt{\langle T\rangle}}{L^4}\int dz\,dz'\int d\boldsymbol{\rho}\,d\boldsymbol{\rho}'\,\varphi_m(z)\\&\times\varphi_{m'}(z')\varphi_{m''}(z)\varphi_{m'''}(z')\delta(\mathbf{r}-\mathbf{r}')\\&=\frac{\beta\sqrt{\langle T\rangle}}{L^2}J_{m,m',m'',m'''},\end{aligned} \tag{A35}$$

with

$$J_{m,m',m'',m'''}(\eta)\equiv\int dz\,\varphi_m(z)\varphi_{m'}(z)\varphi_{m''}(z)\varphi_{m'''}(z). \tag{A36}$$

These integrals were also calculated analytically and tabulated. With the matrix elements $\langle m,m'|V^{\beta}|m'',m'''\rangle$ available, the average repulsive energy per nucleon, $\langle V^{\beta}\rangle$, is calculated in the same way as $\langle V^{\alpha}\rangle$.

Adding equations (A23) and (A24), one obtains the binding energy per nucleon in the slab,

$$B=|\langle T\rangle+\langle V\rangle|, \tag{A37}$$

which is function of $(2M+3)$ variables:

$$B=B(\eta,\rho_G;A_1,A_2,\ldots,A_M;c_0,c_1,\ldots,c_M). \tag{A38}$$

A_0 is not an independent variable due to constraint (14).

[1] A. W. Overhauser, Phys. Rev. Lett. **4**, 415 (1960).
[2] A. E. Pozamantir and A. W. Overhauser, Phys. Rev. C **64**, 014302 (2001), preceding paper.
[3] P. Möller and J. R. Nix, Nucl. Phys. **A549**, 84 (1992).
[4] A. W. Overhauser, Phys. Rev. B **33**, 1468 (1986).
[5] A. W. Overhauser, Phys. Rev. **167**, 691 (1968).